ACS APPLIED MATERIALS & INTERFACES

Research Article

www.acsami.org

The Electrorheological Behavior of Suspensions Based on Molten-Salt Synthesized Lithium Titanate Nanoparticles and Their Core–Shell Titanate/Urea Analogues

T. Plachy,[†,‡] M. Mrlik,[†] Z. Kozakova,[†] P. Suly,[†,‡] M. Sedlacik,*[,†] V. Pavlinek,[†] and I. Kuritka[†]

[†]Centre of Polymer Systems, University Institute, Tomas Bata University in Zlin, Nad Ovcirnou 3685, 760 01 Zlin, Czech Republic

[‡]Polymer Centre, Faculty of Technology, Tomas Bata University in Zlin, Nam. T. G. Masaryka 275, 762 72 Zlin, Czech Republic

ABSTRACT: This paper concerns the preparation of novel electrorheological (ER) materials using microwave-assisted synthesis as well as utilizing a suitable shell-providing system with enhanced ER performance. Lithium titanate nanoparticles were successfully synthesized, and their composition was confirmed via X-ray diffraction. Rheological properties were investigated in the absence as well as in the presence of an external electric field. Dielectric properties clarified the response of the particles to the application of an electric field. The urea-coated lithium titanate nanoparticle-based suspension exhibits higher ER performance in comparison to suspensions based on bare particles.

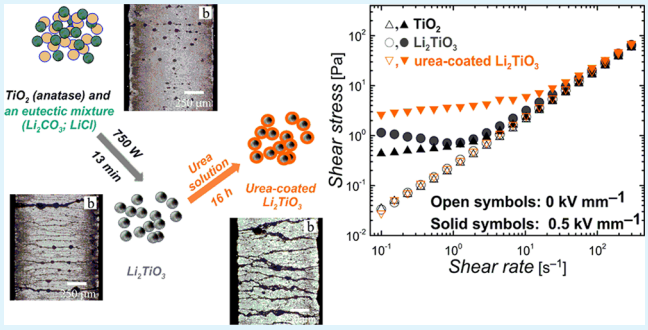

KEYWORDS: *electrorheology, microwave-assisted molten-salt synthesis, anatase, lithium titanate, dielectric properties, steady shear*

1. INTRODUCTION

Electrorheological (ER) suspensions are generally two-phase systems consisting of polarizable particles suspended in an insulating carrier liquid, mostly silicone oil. Such particles are able to create induced dipoles and to form internal chainlike structures after the application of an external electric field. Such structure development results in the transition from a liquid to solid-like state connected to a viscosity increase of several orders of magnitude.[1−8] Hence, ER suspensions have been increasingly applied to the smart control of intelligent as well as conventional devices, such as shock absorbers, clutches, and other applications.[9−11]

Commonly, the dispersed phase is represented by conducting polymers[12−18] or inorganic particles.[19−23] In the case of inorganic particles, many researchers have focused on the synthesis and ER investigation of titanate-based ER suspensions.[24−27] Titanates are preferred due to their high relative permittivity and nanoparticle size contributing to enhanced ER efficiency and substantially improved sedimentation stability.[27,28]

Titanates are mostly prepared by solvothermal synthesis using strong solvents, and reaction times are in the order of hours or days.[24,26] Such procedures are considerably time-consuming and harmful to the environment. On the other hand, molten-salt microwave-assisted synthesis provides a possible way to prepare suitable particles for ER suspensions due to the short reaction times and solvent-free and thus environmentally friendly procedure.[29,30] It has been demonstrated that, by using a molten-salt synthesis, the particle size depends on the temperature and reaction time.[31,32] Usually, the particle size increases with prolonging synthesis time and increasing synthesis temperature.

Hence, this study is focused on the synthesis of lithium titanate (Li-titanate) nanoparticles from titanium dioxide (TiO_2 anatase) nanoparticles via molten-salt microwave-assisted synthesis. The synthesis time was chosen to prepare nanoparticles, since nanoparticles exhibit higher sedimentation stability than micron-sized particles. Moreover, the prepared particles were coated with urea to improve ER performance. Then the rheological properties of the anatase, Li-titanate, and urea-coated Li-titanate-based ER suspensions were investigated in the absence and presence of an external electric field. The interfacial polarization mostly responsible for the ER effect was then evaluated through a dielectric property examination.

2. EXPERIMENTAL SECTION

2.1. Synthesis of Lithium Titanate Nanoparticles. Li-titanate particles were prepared by molten-salt synthesis without the use of any solvent. A mixture of reactants, that is, 1 g of TiO_2 anatase, 2.47 g of lithium chloride, and 1.53 g of lithium carbonate (all purchased from Sigma-Aldrich, USA), was homogenized in a mortar and inserted into a corundum crucible. The filled crucible was placed into a special ceramic kiln, the inner walls of which were coated with graphite. Then the kiln was put into a common domestic microwave oven working at frequency 2.45 GHz and a maximum power of 750 W. The reacting mixture was treated for 20 min at maximum power and then allowed to cool to room temperature inside the closed ceramic kiln. Then, the

Received: December 2, 2014
Accepted: January 29, 2015
Published: January 29, 2015

DOI: 10.1021/am508471f
ACS Appl. Mater. Interfaces 2015, 7, 3725−3731

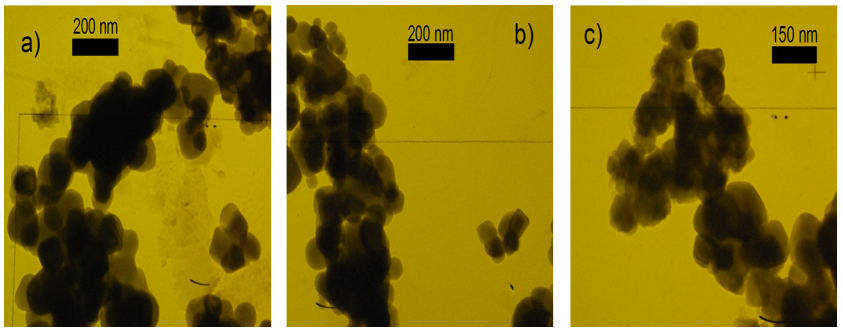

Figure 1. TEM images for (a) TiO_2 anatase, (b) S1, and (c) S2 particles.

obtained compact solid product was rinsed with demineralized water, removed by filtration, and then washed with demineralized water again. The product was labeled as Sample 1 (S1) and then dried in an oven under vacuum at 60 °C to a constant weight.

2.2. Treatment of S1 Particles in Urea Solution. The prepared S1 particles (1.5 g) were immersed in 50 mL of demineralized water at 45 °C. After 1 h, 1.5 mL of 10 wt % aqueous solution of urea (Sigma-Aldrich, USA) was added. The mixture was stirred for another 16 h. Subsequently, the suspension was filtered and rinsed with demineralized water. The obtained particles were dried in a vacuum oven at 60 °C to a constant weight. These particles were then labeled as Sample 2 (S2).

2.3. Characterization of Prepared Nanoparticles. The morphology and dimensions of the particles were observed using transmission electron microscopy (TEM; Tesla 500, Czech Republic). The chemical composition of the prepared titanate particles was characterized with the use of X-ray diffraction (XRD) analysis. The diffraction pattern of the prepared material was examined using an X-pert PRO (Phillips, The Netherlands) diffractometer with a Cu Kα_1 radiation (λ = 0.154 nm) and a scanning rate of 4 min^{-1} in an angle range of 10−95° 2θ. To confirm the presence of urea in the S2 and to determine its amount, Fourier transform infrared spectra were measured via the ATR method with a diamond crystal in a range of 4000−500 cm^{-1} on a Nicolet 6700 (Nicolet, USA). A thermogravimetric analysis (TGA; TGA Q500; TA Instruments, USA) was also made. The TGA measurement was performed at a heating rate of 5 °C min^{-1} from 25 to 400 °C under a nitrogen atmosphere.

TEM images (Figure 1a−c) show agglomerates of (a) the precursor material TiO_2 anatase, (b) the prepared S1, and (c) the prepared S2. The particles possess a spherical shape with a diameter in the range between tens of nanometres to 150 nm indicating that samples S1 and S2 belong to the group of nanoparticles. It can be seen that the prepared S1 and S2 particles have similar dimensions to those of the TiO_2 anatase particles.

On the basis of a comparison with the ICDD PDF-2 database, the prevailing crystallographic phase present in the sample was identified as Li_2TiO_3 (Figure 2). The compound Li_2TiO_3 crystallizes in three structural modifications, cubic α-Li_2TiO_3 (space group $Fm\bar{3}m$), which is metastable and above 300 °C transforms irreversibly into the monoclinic β-Li_2TiO_3 (space group $C2/c$). The monoclinic phase is stable in a wide temperature range up to 1150 °C, after which cubic γ-Li_2TiO_3 (space group $Fm\bar{3}m$) occurs. The diffraction patterns of the monoclinic and cubic crystallographic phases contain several peaks presented in the same position; however, the complex character of the diffraction pattern of S1 presented in Figure 2 contains diffraction peaks in the range of 2θ angles from 20 to 24°, which are specific just for the monoclinic phase and thus indicate the presence of this phase in the prepared material. This can also be supported by the fact that the temperature of synthesis is assumed to be in the range of ∼600−800 °C, in which the monoclinic phase is stable.

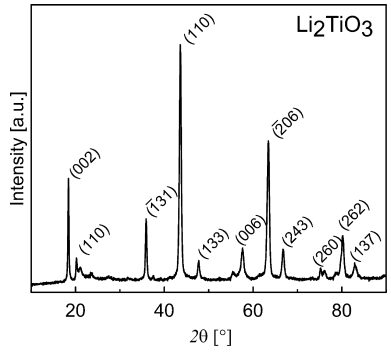

Figure 2. Powder XRD pattern of synthesized S1 particles.

In Figure 3, the FTIR spectra of the bare S1 particles and also the particles after urea coating can be seen. The particles before coating

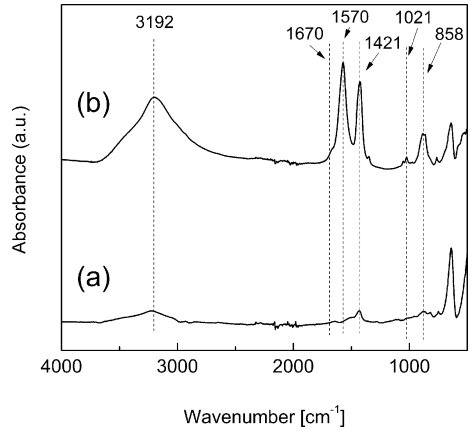

Figure 3. FTIR spectra for S1 (a) and S2 (b).

(S1) exhibit typical stretching vibrations for −OH groups at 3200 cm^{-1} and typical vibrations at 1421 and 858 cm^{-1} and lower for TiO_3 bands.[33] Further, in the case of urea-modified particles (S2), the typical N−C−N asymmetric and symmetric stretching vibrations at 1421 and 1021 cm^{-1} are presented, respectively. Also the C═O stretching and N−H bending appear at 1670 and 1570 cm^{-1}.[34] The broad band at 3192 cm^{-1} can be attributed to the N−H stretching and/or O−H stretching in adsorbed water. The broadening of this peak can be also assigned to the enhanced interaction of the S1 with urea by hydrogen bonding, as was also observed by Cheng et al.[35]

The presence of urea on the surface of S1 after its treatment was also confirmed by TGA. The TGA curve for S2 (Figure 4) exhibits a similar shape to the curve obtained for pure urea.[36] The highest mass loss was observed in the temperature region of ∼150−260 °C. By TGA analysis, it was confirmed that the amount of urea present in S2 was 1.86%. The first step may be attributed to the partial decomposition of urea to isocyanic acid and ammonia. The less-developed peak in differential TGA and the low loss of mass above the temperature 260 °C represents residual byproducts of urea decomposition like ammelide or cyanuric acid. The further decrease

DOI: 10.1021/am508471f
ACS Appl. Mater. Interfaces 2015, 7, 3725−3731

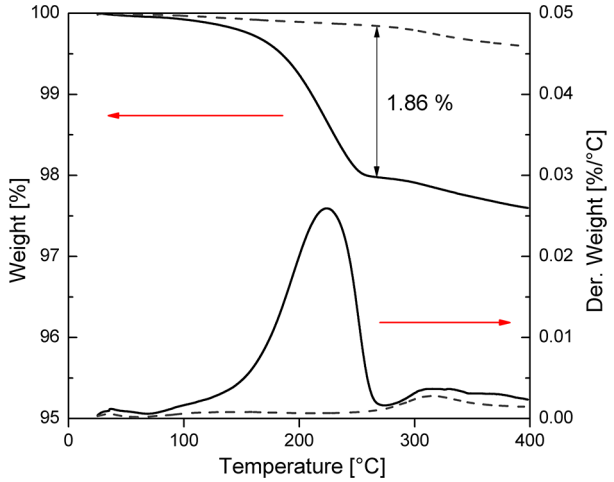

Figure 4. TGA analysis of S1 (dashed line) and S2 (solid line) samples.

in mass represents the decomposition of cyanuric acid.[36] It is also seen that bare S1 particles are stable up to 400 °C, and the mass change is significantly smaller in comparison with S2.

2.4. Preparation of Electrorheological Suspensions. The prepared particles were dried in a vacuum oven at 60 °C for 24 h. Subsequently, ER suspensions of concentration 5, 10, and 15 wt % were prepared by mixing the dried particles with silicone oil (Lukosiol M200, Chemical Works Kolín, Czech Republic, viscosity η_c = 194 mPa s, conductivity $\sigma_c \approx 10^{-11}$ S cm^{-1}), which were then dried under the same conditions. The suspensions were stirred manually for 5 min and then sonicated for 1 min before each measurement.

2.5. Electrorheological Measurements. Steady shear measurements in controlled shear rate mode were carried out using a Bohlin Gemini rotational rheometer (Malvern Instruments, U.K.) with parallel plate geometry 40 mm in diameter and a gap of 0.5 mm. A DC TREK 668B high-voltage source (TREK, USA) was used for the generation of external electric fields of strength 0−3 kV mm^{-1}. Before each measurement, and the suspension was sheared for 60 s at a shear rate of 40 s^{-1} to destroy residual chainlike structures. In the case of measurements in the presence of an electric field, the electric field was applied for 60 s before shearing to provide enough time for particles to create organized structures within the suspensions.

2.6. Dielectric Properties. Dielectric properties of prepared suspensions were measured with an impedance analyzer (4294A, Agilent Technologies, Japan) connected to a cell for liquid materials (16482A, Agilent Technologies, Japan). Dielectric properties such as relative permittivity, ε', and dielectric loss factor, ε'', were investigated in a frequency range from 60 Hz to 2 MHz. Dielectric spectra were analyzed using the Havriliak−Negami (H−N) model[37]

$$\varepsilon^*_{HN}(\omega) = \varepsilon'_\infty + \frac{\Delta\varepsilon'}{(1 + (i\omega \cdot t_{rel})^a)^b} \quad (1)$$

where $\Delta\varepsilon' = \varepsilon'_s - \varepsilon'_\infty$ is the dielectric relaxation strength, ε'_s and ε'_∞ are the relative permittivities at zero and infinite frequency f, respectively, ω is the angular frequency ($=2\pi f$), t_{rel} is the relaxation time, and a and b are shape parameters describing the asymmetry of the dielectric function.

2.7. Optical Microscopy. Suspensions consisting of 1 wt % of particles in silicone oil were placed between two copper electrodes deposited on a glass (gap of 1 mm) connected to a DC high-voltage source (Keithley 2400, USA). The formation of ER structures was observed with the help of an optical microscope (N 400M, China) linked to a digital camera.

3. RESULTS AND DISCUSSION

3.1. Electrorheological Properties. The ER performance of 5 wt % suspensions based on TiO_2 anatase and S1 was investigated in the absence and in the presence of an electric field. As can be seen in Figure 5, the suspensions exhibit

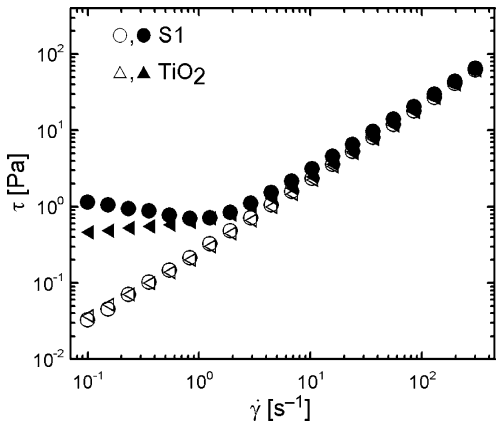

Figure 5. Dependence of shear stress τ on shear rate $\dot{\gamma}$ for 5 wt % ER suspensions based on TiO_2 anatase and S1 particles in the absence (○, △) and in the presence (●, ▲) of an external electric field of a strength of 3 kV mm^{-1}.

Newtonian behavior in the absence of an electric field, and their field-off viscosity is similar. However, in the presence of an electric field of a strength of 3 kV mm^{-1}, the S1-based suspension shows a higher yield stress than the anatase-based suspension due to the increased polarizability of the S1 particles. At shear rates above 10 s^{-1}, the shear stress of both suspensions started to exhibit values regardless of whether the external electric field is applied or not (Figure 5). The values of shear stress of ER suspensions in the presence of external electric field are determined by the ratio of electrostatic and hydrodynamic forces. Since the loading of the suspensions is only 5 wt %, the electrostatic forces are weak, and hydrodynamic ones start to dominate over them at quite low shear rates. Similar values of shear stress were then obtained due to similar particle size of both suspensions. Very similar behavior has been observed with an ER suspension based on particles of low conductivity.[38,39]

Because of the increased yield stress, the S1 sample seems to be a more promising material for a highly effective ER fluid in comparison with the TiO_2 anatase. These findings were also confirmed via observation of the structure development under the application of an external electric field (see Section 3.3, Structure Development under DC Electric Field). The S1 particles were therefore further treated in urea solution to improve the ER performance of their silicone oil suspensions.

Figure 6 shows the ER performance of suspensions containing various concentrations of S2 particles. The suspension containing 5 wt % particles behaves as a Newtonian fluid in the absence of an electric field and exhibits higher yield stress at the same electric field strength than the suspension based on S1 particles in Figure 5. Thus, the introduction of a polar layer on the surface of S1 led to an increase in the ER effect of the suspension. The suspensions based on 10 and 15 wt % particles behave rather like pseudoplastic fluids than Newtonian ones in the absence of an electric field. However, upon the application of an external electric field strength of 3 kV mm^{-1}, both begin to act as Bingham fluids exhibiting considerable high-yield stresses. The higher particle concentration in the suspensions led to a significant increase in the ER effect of these suspensions; the particles were able to create

DOI: 10.1021/am508471f
ACS Appl. Mater. Interfaces 2015, 7, 3725−3731

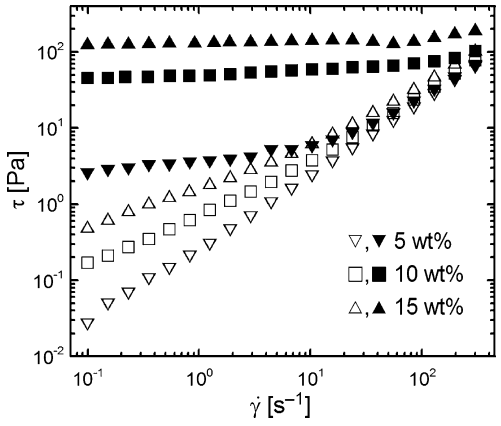

Figure 6. Dependence of shear stress τ on shear rate $\dot{\gamma}$ for the ER suspensions based on the various concentrations of S2 in the absence (△, □, ▽) and in the presence (▲, ■, ▼) of an external electric field of a strength of 3 kV mm^{-1}.

stiffer and tougher chainlike structures than in the case of suspensions with a low loading of the particles.

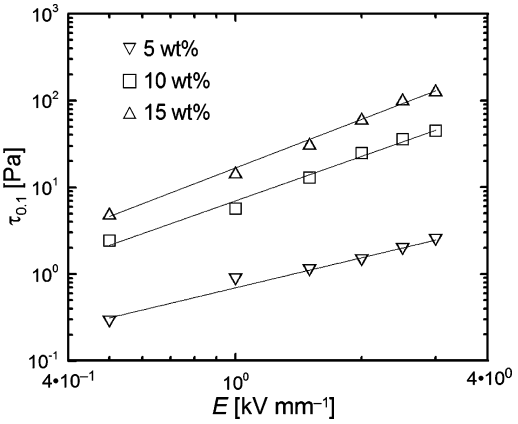

Figure 7. Values of the shear stress obtained at the shear rate 0.1 s^{-1} vs the electric field strength for the ER suspensions based on various concentrations of S2.

It was proposed that the log−log dependence of the yield stress on the electric field strength (Figure 7) obeys the power law

$$\tau = q \times E^{\alpha} \quad (2)$$

where q represents the rigidity of the internal structures created upon the application of the electric field, and the value of parameter α should be within the range of 1.5−2 for well-developed structures.[40,41] However, since it is complicated to exactly determine the yield stress, the values of shear stress at a very low shear rate of 0.1 s^{-1} were taken for this evaluation. In the case of suspensions based on 15 and 10 wt % S2 particles, their α parameters possess values of 1.87 and 1.70, respectively. This indicates better-developed structures upon application of the external electric field for the higher-loaded suspension. Thus, the increased amount of polarizable particles leads to the creation of a stiffer system exhibiting a higher ER effect. For the suspension based on 5 wt % S2 particles, the α parameter is only 1.15, which corresponds well with the low ER effect of this suspension.

From the application point of view, the difference between viscosity in the presence of an external electric field η_E and viscosity in the absence of an electric field η_0 is of high importance. This difference is embodied in the formula of ER efficiency e, where

$$e = (\eta_E - \eta_0)/\eta_0 \quad (3)$$

Figure 8 shows the dependence of ER efficiency on the shear rate for the S2 sample suspensions. Despite the highest field-off

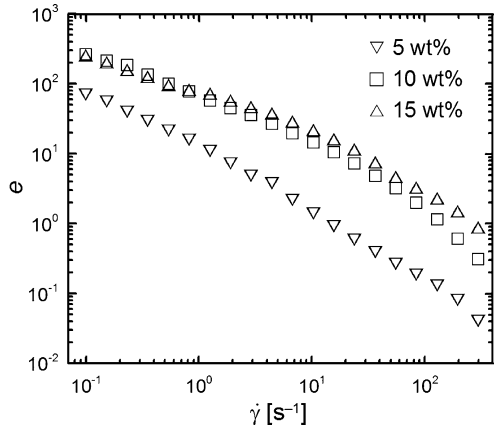

Figure 8. Dependence of the ER efficiency e on the shear rate $\dot{\gamma}$ for the ER suspensions based on the various concentrations of S2.

viscosity, the suspension based on 15 wt % S2 particles exhibits the highest ER efficiency together with the suspension based on 10 wt % S2 particles. However, it can be seen that at higher shear rates than 10^{-1} s, a higher efficiency for the suspension based on 15 wt % S2 particles is observed. This is a consequence of the changes in the field-off viscosity with increasing shear rates. The higher-loaded suspension behaves more like a pseudoplastic fluid; thus, its viscosity is significantly higher than the viscosity of the suspension containing 10 wt % S2 particles. However, at shear rates higher than 10^{-1} s, the difference significantly decreases and is similar for both suspensions, which leads to the higher efficiency of the suspension based on 15 wt % S2 particles due to its higher ER effect. The suspension based on 5 wt % S2 particles, which possesses the lowest field-off viscosity, exhibits also the lowest ER efficiency. This corresponds well with its ER effect (lower by more than 1 order of magnitude) in comparison with both higher-loaded suspensions. It can also be assumed that a further increase in the concentration of S2 particles in the suspensions would not lead to an ER fluid with higher ER efficiency owing to the high increase of field-off viscosity.

3.2. Dielectric Properties. Generally, interfacial polarization is mostly responsible for the formation of the internal structures in the ER suspensions.[42−45] In the dielectric spectra (Figure 9), the presence of the relaxation peaks of both S1 and S2 5 wt %-based suspensions can be clearly seen. From an investigation of these spectra by an H−N model fit, the suitability of the synthesized S1 and S2 nanoparticles as dispersed phases in ER suspensions can be evaluated. The parameters of H−N model fits are shown in Table 1. Relaxation time t_{rel} and dielectric relaxation strength $\Delta\varepsilon'$ are the most important. Here the relaxation time reflects the rate of the

DOI: 10.1021/am508471f
ACS Appl. Mater. Interfaces 2015, 7, 3725−3731

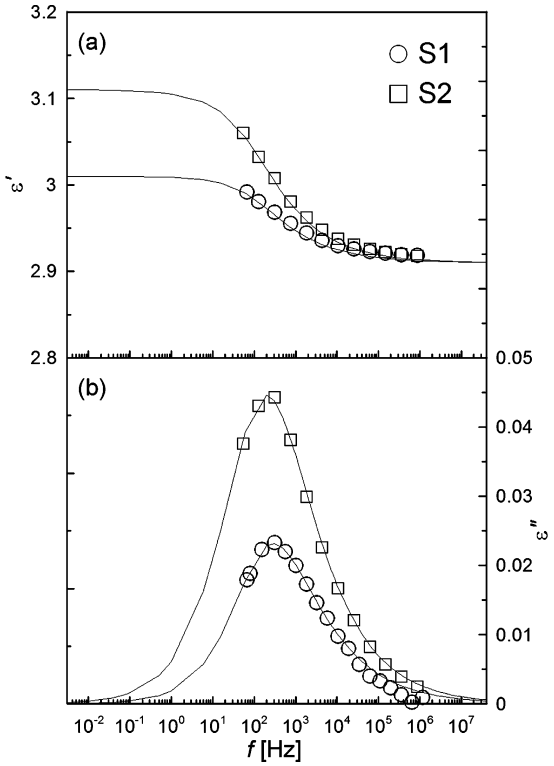

Figure 9. Frequency dependence of relative permittivity ε' (a) and dielectric loss factor ε'' (b) for 5 wt % silicone oil ER suspensions. Solid lines represent the Havriliak–Negami model fit.

Table 1. Parameters of the Havriliak–Negami Model Fit for the 5 wt % Suspensions of S1 and S2 Nanoparticles

sample name	ε'_s	ε''_∞	$\Delta\varepsilon'$	t_{rel} [s]	a	b
S1	3.01	2.91	0.10	1.15×10^{-3}	0.66	0.59
S2	3.11	2.91	0.20	1.49×10^{-3}	0.61	0.68

interfacial polarization, which is on the same level for both investigated systems. However, dielectric relaxation strength as a measure of the electrostatic interactions between particles is two times higher for the S2-based suspension. Hence, the introduction of polar urea groups on the surface of S1 provides particles with higher polarizability, and their suspensions exhibit enhanced ER performance.

3.3. Structure Development under Direct Current Electric Field. To properly investigate the internal structure formation under the presence of an external electric field, the micrographs of structures (Figures 10 and 11) were analyzed. Since the small particles with high surface areas possess high surface energy, they tend to join together in bigger agglomerates; therefore, it was possible to investigate their structure by optical microscopy. The small amount of the original TiO_2 anatase agglomerates is randomly dispersed in the absence of an external electric field (Figure 10a). After the application of the external electric field of 1.5 kV mm^{-1}, the TiO_2 anatase agglomerates are concentrated around the electrodes, and only large agglomerates developing defective structures are partially oriented (Figure 10b). On the other hand, S1 small agglomerates randomly dispersed in silicone oil in the absence of an external field (Figure 11a) are able to create considerably better-developed internal structures after the application of the same electric field strength (Figure 11b). Created agglomerates form visible chainlike internal structures and consequently provide enhanced ER activity well-reflected in the rheological behavior. The highest ER activity was observed for the suspension based on S2. The particles are also randomly dispersed in the silicone oil in the absence of an external electric field (Figure 12a). However, after its application the particles undergo a transition to highly organized, oriented, chainlike structures in the direction of the applied electric field (Figure 12b). The resulting structures are obviously better formed than in the previous cases due to their enhanced dielectric relaxation strength. Therefore, the suspension based on S2 exhibits the highest ER effect among these suspensions.

CONCLUSIONS

In this paper the simple and fast preparation of lithium titanate nanoparticles via microwave-assisted molten-salt synthesis was presented. To improve the behavior of the bare lithium titanate nanoparticles under applied external electric field, these particles were coated with urea. It was observed that a suspension based on urea-coated particles exhibits a higher yield stress in 2 orders of magnitude in comparison to the bare ones. With higher particle concentration in the suspensions, higher ER effect was exhibited. While the relaxation times of the suspensions were nearly the same for both, the dielectric relaxation strength was 2 times higher for the suspension based on urea-coated particles than for the suspension based on the bare ones. This explains the increased ER effect of the suspension based on urea-coated particles. Optical microscopy observation provides images well-corresponding with the previous ER findings and consequently shows the suitability of the presented method for the preparation of electrically

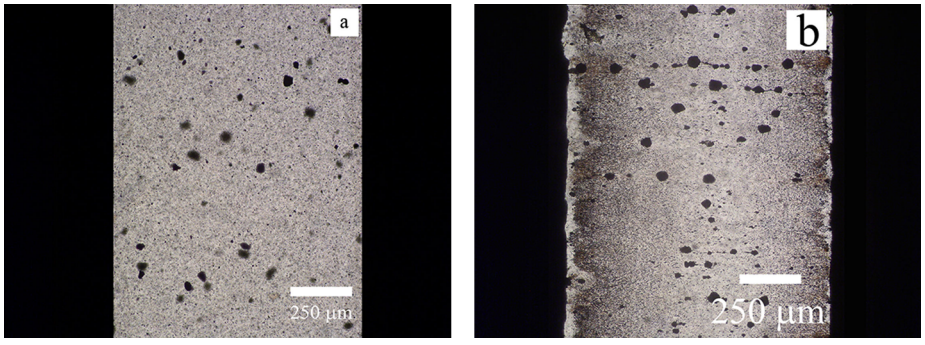

Figure 10. Optical microscopy of a 1 wt % silicone oil suspension of TiO_2 anatase nanoparticles under various electric field strengths E (kV mm^{-1}): (a) 0, (b) 1.5.

DOI: 10.1021/am508471f
ACS Appl. Mater. Interfaces 2015, 7, 3725–3731

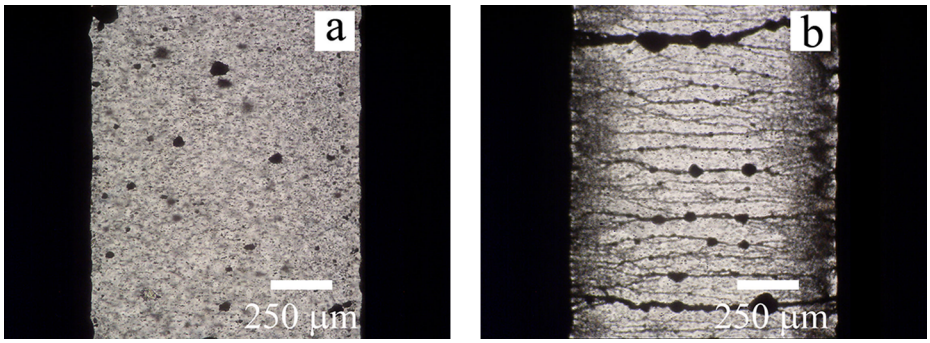

Figure 11. Optical microscopy of a 1 wt % silicone oil suspension of S1 nanoparticles under various electric field strengths E (kV·mm^{-1}): (a) 0, (b) 1.5.

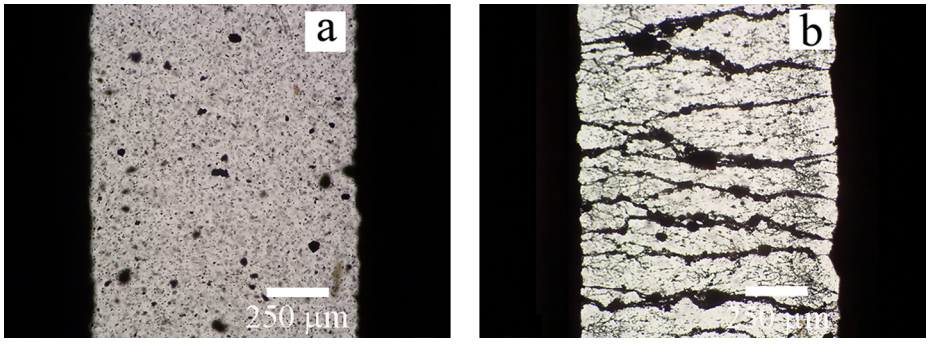

Figure 12. Optical microscopy of 1 wt % silicone oil suspension of S2 nanoparticles under various electric field strengths E (kV·mm^{-1}): (a) 0, (b) 1.5.

polarizable particles from TiO_2 anatase nanoparticles for novel ER suspension.

AUTHOR INFORMATION

Corresponding Author

*E-mail: msedlacik@ft.utb.cz.

Notes

The authors declare no competing financial interest.

ACKNOWLEDGMENTS

This article was written with the support of the Operational Program Research and Development for Innovations cofunded by the European Regional Development Fund (ERDF) and the national budget of the Czech Republic, within the framework of the project of the Centre of Polymer Systems (Reg. No. CZ.1.05/2.1.00/03.0111). Further, T.P. is thankful for an internal grant from TBU in Zlin, No. IGA/FT/2013/014, funded from specific university research resources.

REFERENCES

(1) Alanis, E.; Romero, G.; Martinez, C.; Alvarez, L.; Mechetti, M. Characteristic times of microsturcture formation in electrorheological fluids, determined by viscosity and speckle activity measurements. *Appl. Rheol.* **2005**, *15* (1), 38−45.

(2) Block, H.; Kelly, J. P. Electro-Rheology. *J. Phys. D: Appl. Phys.* **1988**, *21* (12), 1661−77.

(3) Gast, A. P.; Zukoski, C. F. Electrorheological Fluids as Colloidal Suspensions. *Adv. Colloid Interface Sci.* **1989**, *30* (3−4), 153−202.

(4) Hao, T. Electrorheological fluids. *Adv. Mater.* **2001**, *13* (24), 1847−57.

(5) Menna, T. J.; Filisko, F. E.; Lynch, R. A. Effect of electric fields on the rheological properties of the isotropic phase of phic/p-xylene solutions. *Appl. Rheol.* **2005**, *15* (3), 172−6.

(6) Stenicka, M.; Pavlinek, V.; Sahaha, P.; Blinova, N. V.; Stejskal, J. Quadrat O. Electrorheology of suspensions of variously protonated polyaniline particles under steady and oscillatory shear. *Appl. Rheol.* **2010**, *20* (5), 1−11.

(7) Schneider, S.; Eibl, S. Review of the electrorheological (ER) effect of polyurethane-based ER fluids. *Appl. Rheol.* **2008**, *18* (2), 8.

(8) Plachy, T.; Sedlacik, M.; Pavlinek, V.; Trchová, M.; Morávková, Z.; Stejskal, J. Carbonization of aniline oligomers to electrically polarizale particles and their use in electrorheology. *Chem. Eng. J.* **2014**, *256*, 398−406.

(9) Parthasarathy, M.; Klingenberg, D. J. Electrorheology: Mechanisms and models. *Mater. Sci. Eng., R.* **1996**, *17* (2), 57−103.

(10) Tang, H.; Zhao, X. P.; Wang, B. X.; Zhao, Y. Response characteristics of a viscoelastic gel under the co-action of sound waves and an electric field. *Smart Mater. Struct.* **2006**, *15* (1), 86−92.

(11) Weiss, K. D.; Carlson, J. D.; Nixon, D. A. Viscoelastic Properties of Magnetorheological and Electrorheological Fluids. *J. Intell. Mater. Syst. Struct.* **1994**, *5* (6), 772−5.

(12) Hong, C. H.; Choi, H. J. Shear stress and dielectric analysis of H3PO4 doped polyaniline based electrorheological fluid. *J. Macromol. Sci., Part B: Phys.* **2007**, *46* (4), 683−92.

(13) Cheng, Q. L.; Pavlinek, V.; He, Y.; Yan, Y. F.; Li, C. Z.; Saha, P. Template-free synthesis of hollow poly(*o*-anisidine) microspheres and their electrorheological characteristics. *Smart Mater. Struct.* **2011**, *20* (6), 6.

(14) Choi, S. B.; Choi, H. J.; Choi, Y. T.; Wereley, N. M. Preparation and mechanical characteristics of poly(methylaniline) based electrorheological fluid. *J. Appl. Polym. Sci.* **2005**, *96* (5), 1924−9.

(15) Lengalova, A.; Pavlinek, V.; Cheng, Q. L.; Saha, P. Increasing electrorheological response of particles: The effect of conductive polymer. *Int. J. Mod. Phys. B* **2007**, *21* (28−29), 4883−9.

(16) Pavlinek, V.; Saha, P.; Perez-Gonzalez, J.; de Vargas, L.; Stejskal, J. Quadrat O. Analysis of the yielding behavior of electrorheological suspensions by controlled shear stress experiments. *Appl. Rheol.* **2006**, *16* (1), 14−8.

DOI: 10.1021/am508471f
ACS Appl. Mater. Interfaces 2015, 7, 3725−3731

(17) Stenicka, M.; Pavlinek, V.; Saha, P.; Blinova, N. V.; Stejskal, J. Quadrat O. Structure changes of electrorheological fluids based on polyaniline particles with various hydrophilicities and time dependence of shear stress and conductivity during flow. *Colloid Polym. Sci.* **2011**, *289* (4), 409−14.
(18) Stenicka, M.; Pavlinek, V.; Saha, P.; Blinova, N. V.; Stejskal, J. Quadrat O. The effect of compatibility of suspension particles with the oil medium on electrorheological efficiency. *J. Intell. Mater. Syst. Struct.* **2012**, *23* (9), 1055−9.
(19) Cheng, Q. L.; Pavlinek, V.; He, Y.; Lengalova, A.; Li, C. Z.; Saha, P. Structural and electrorheological properties of mesoporous silica modified with triethanolamine. *Colloids Surf., A* **2008**, *318* (1−3), 169−74.
(20) Cheng, Q. L.; Pavlinek, V.; He, Y.; Yan, Y. F.; Li, C. Z.; Saha, P. Synthesis and electrorheological characteristics of sea urchin-like TiO_2 hollow spheres. *Colloid Polym. Sci.* **2011**, *289* (7), 799−805.
(21) Liu, Y. D.; Choi, H. J. Electrorheological fluids: smart soft matter and characteristics. *Soft Matter* **2012**, *8* (48), 11961−78.
(22) Mrlik, M.; Pavlinek, V.; Saha, P. Quadrat O. Electrorheological Properties of Suspensions of Polypyrrole-Coated Titanate Nanorods. *Appl. Rheol.* **2011**, *21* (5), 7.
(23) Zhao, X. P.; Yin, J. B. Advances in electrorheological fluids based on inorganic dielectric materials. *J. Ind. Eng. Chem.* **2006**, *12* (2), 184−98.
(24) He, Y.; Cheng, Q. L.; Pavlinek, V.; Li, C. Z.; Saha, P. Synthesis and electrorheological characteristics of titanate nanotube suspensions under oscillatory shear. *J. Ind. Eng. Chem.* **2009**, *15* (4), 550−4.
(25) Cheng, Q. L.; Pavlinek, V.; He, Y.; Li, C. Z.; Saha, P. Electrorheological characteristics of polyaniline/titanate composite nanotube suspensions. *Colloid Polym. Sci.* **2009**, *287* (4), 435−41.
(26) Yin, J. B.; Zhao, X. P. Preparation and electrorheological characteristic of Y-doped BaTiO3 suspension under dc electric field. *J. Solid State Chem.* **2004**, *177* (10), 3650−9.
(27) Yin, J. B.; Zhao, X. P. Titanate nano-whisker electrorheological fluid with high suspended stability and ER activity. *Nanotechnology* **2006**, *17* (1), 192−6.
(28) Lee, B. M.; Kim, J. E.; Fang, F. F.; Choi, H. J.; Feller, J. F. Rectangular-Shaped Polyaniline Tubes Covered with Nanorods and their Electrorheology. *Macromol. Chem. Phys.* **2011**, *212* (21), 2300−7.
(29) Kozakova, Z.; Mrlik, M.; Sedlacik, M.; Pavlinek, V.; Kuritka, I. Preparation of TiO_2 Powder by Microwave-Assisted Molten-Salt Synthesis. In *Nanocon 2011;* Tanger Ltd: Slezska, 2011; pp 345−51.
(30) Sedlacik, M.; Mrlik, M.; Kozakova, Z.; Pavlinek, V.; Kuřitka, I. Synthesis and electrorheology of rod-like titanium oxide particles prepared via microwave-assisted molten-salt method. *Colloid Polym. Sci.* **2012**, *290* (2), 1−7.
(31) Lu, Z. Y.; Wang, Y. L.; Wu, W. J.; Li, Y. X. Morphology and structure of $LiNb_{0.6}Ti_{0.5}O_3$ particles by molten salt synthesis. *J. Alloy. Compd.* **2011**, *509* (40), 9696−701.
(32) Zhang, Z. Q.; Liu, Z. F.; Li, Y. X. Influence of synthesis conditions on the microstructure of Li-Ta-Ti-O microsheets by molten salt method. *Ceram. Int.* **2014**, *40* (2), 3747−53.
(33) Cheng, Q. L.; He, Y.; Pavlinek, V.; Li, C. Z.; Saha, P. Surfactant-assisted polypyrrole/titanate composite nanofibers: Morphology, structure and electrical properties. *Synth. Met.* **2008**, *158* (21−24), 953−7.
(34) Liu, Y. D.; Lee, B. M.; Park, T. S.; Kim, J. E.; Choi, H. J.; Booh, S. W. Optically transparent electrorheological fluid with urea-modified silica nanoparticles and its haptic display application. *J. Colloid Interface Sci.* **2013**, *404*, 56−61.
(35) Cheng, Q. L.; Pavlinek, V.; He, Y.; Li, C. Z.; Lengalova, A.; Saha, P. Facile fabrication and characterization of novel polyaniline/titanate composite nanotubes directed by block copolymer. *Eur. Polym. J.* **2007**, *43* (9), 3780−6.
(36) Brack, W.; Heine, B.; Birkhold, F.; Kruse, M.; Schoch, G.; Tischer, S.; et al. Kinetic modeling of urea decomposition based on systematic thermogravimetric analyses of urea and its most important by-products. *Chem. Eng. Sci.* **2014**, *106*, 1−8.
(37) Havriliak, S.; Negami, S. A Complex Plane Representation of Dielectric and Mechanical Relaxation Processes in Some Polymers. *Polymer* **1967**, *8* (4), 161−72.
(38) Mrlik, M.; Sedlacik, M.; Pavlinek, V.; Bober, P.; Trchova, M.; Stejskal, J.; et al. Electrorheology of aniline oligomers. *Colloid Polym. Sci.* **2013**, *291* (9), 2079−86.
(39) Liu, Y. D.; Kim, J.; Ahn, W. S.; Choi, H. J. Novel electrorheological properties of a metal-organic framework Cu-3(BTC)(2). *Chem. Commun.* **2012**, *48* (45), 5635−7.
(40) Davis, L. C. Time-dependent and nonlinear effects in electrorheological fluids. *J. Appl. Phys.* **1997**, *81* (4), 1985−91.
(41) Kim, S. G.; Lim, J. Y.; Sung, J. H.; Choi, H. J.; Seo, Y. Emulsion polymerized polyaniline synthesized with dodecylbenzenesulfonic acid and its electrorheological characteristics: Temperature effect. *Polymer* **2007**, *48* (22), 6622−31.
(42) Lengalova, A.; Pavlinek, V.; Saha, P. Quadrat O, Kitano T, Steiskal J. Influence of particle concentration on the electrorheological efficiency of polyaniline suspensions. *Eur. Polym. J.* **2003**, *39* (4), 641−5.
(43) Mrlik, M.; Pavlinek, V.; Cheng, Q. L.; Saha, P. Synthesis of Titanate/Polypyrrole Composite Rod-Like Particles and the Role of Conducting Polymer on Electrorheological Efficiency. *Int. J. Mod. Phys. B* **2012**, *26* (2), 8.
(44) Yin, J. B.; Zhao, X. P. Electrorheological properties of titanate nanotube suspensions. *Colloids Surf., A* **2008**, *329* (3), 153−60.
(45) Zhang, W. L.; Liu, Y. D.; Choi, H. J.; Kim, S. G. Electrorheology of Graphene Oxide. *ACS Appl. Mater. Interfaces* **2012**, *4* (4), 2267−72.

DOI: 10.1021/am508471f
ACS Appl. Mater. Interfaces 2015, 7, 3725−3731